A LOCAL MESHLESS RBF METHOD FOR SOLVING FRACTIONAL INTEGRO-DIFFERENTIAL EQUATIONS WITH OPTIMAL SHAPE PARAMETERS

Mehdi Safinejad*
Department of Mathematics
Faculty of Sciences and Modern Technology
Graduate University of Advanced Technology
Kerman
Iran
m.safinejad@gmail.com

Mahmoud Mohseni Moghaddam
Department of Mathematics
Faculty of Sciences and Modern Technology
Graduate University of Advanced Technology
Kerman
Iran
mohseni@uk.ac.ir

Abstract. This paper investigates the application of the meshless local radial basis functions collocation method (LRBFCM) for the numerical solution of fractional integro-differential equation and two-dimensional fractional Volterra integral equation. Unlike the traditional global RBF collocation method, dividing the collocation of the problem in the global domain into many local regions, and therefore, the ill-conditioning of the problem is reduced and becomes highly stable. Here, we use the multiquadric (MQ) radial basis function that includes a shape parameter, which plays an important role in the accuracy of method. Scaling of the shape parameter to make local RBF approximation insensitive is performed by particle swarm optimization (PSO) algorithm. Some test problems are studied and the numerical results shows the efficiency of the method.

Keywords: fractional calculus, local meshless methods, fractional integral-differential equations, collocation methods, optimal shape parameter.

1. Introduction

Meshless methods are very attractive and effective for solving boundary value problems, because they involve simple preprocessing, arbitrary node distribution and flexibility of placing nodes at arbitrary locations. Also, they are easily extendable to higher dimensional problems. These methods may use strong form [1, 2, 3] or weak form of governing equations [4, 5, 6, 7]. Also, these methods may treat the problem locally [8, 9, 10, 11] or globally [12]. Since the final matrix ob-

∗. Corresponding author

tained in global methods are usually full and ill conditioned, local methods were proposed in the literature. Local multiquadric approximation (LMQ) method [13, 8, 14] and the finite collocation approach (FC) [9, 15] are among the popular local methods which use strong form equations. These local methods reduce the problem into many local sub-problems and finally assemble all these local equations into the final global matrix. Therefore, the final global matrix obtained by LMQ and FC methods are sparse. In this paper we use the multiquadric (MQ) radial basis function. Kansa [16] applied MQ functions for scattered data approximation in and presented a new approach to solve PDEs [17]. MQ was employed as a spatial approximation scheme for Hyperbolic, parabolic and the elliptic Poisson's equation. This function has a free parameter (c) called shape parameter. This parameter plays an important role for the accuracy of the method, and is achieved by various techniques. The particle swarm optimization (PSO) algorithm is applied to obtain the optimum value of this parameter. In this paper our aim is to suggest and apply the local RBF method based on multi-quadratics for the numerical solutions of the fractional integro-differential equation and fractional integral equations. These equations form an important part of applied mathematics, which links with many theoretical and practical fields. The concept of the fractional derivative was introduced in the middle of the 19th century by Riemann and Liouville. Many physical and biological models are formulated using fractional differentials. So, in recent years the number of publications about the fractional calculus has rapidly increased [4, 11, 18]. This paper is organized as follows: In Section 2, the basic defnitions in fractional calculus and fractional integral equation which is needed in the next sections are presented. In Section 3, the local RBF method for discretizing fractional integral and integro-differential equations is described. Section 4 is devoted to introducing particle swarm optimization algorithm for finding optimal shape parameters. Numerical results are given in Section 5. Our conclusions are summerized in Section 6.

2. Basic definitions

In this section, we give some basic deffnitions and properties of the fractional calculus theory which are used further in this paper [18, 19].

Let $f(x)$ be a function defined on (a, b), then we have the following definitions:

Definition 1. The Riemann-Liouville(R-L) fractional integration operator of order $\alpha \geq 0$ of a function f is defined as:

$$I^{\alpha} f(x) = \begin{cases} \frac{1}{\Gamma(\alpha)} \int_a^x \frac{f(t)}{(x-t)^{1-\alpha}} dt, & \alpha > 0,\ x > 0, \\ f(x), & \alpha = 0, \end{cases}$$

where $\Gamma(.)$ is the gamma function and I is the fractional integral.

Definition 2. The Riemann - Liouville fractional derivative of $f(x)$ is:

$$ {}^{R}D^{\alpha}f(x) = \begin{cases} \frac{1}{\Gamma(m-\alpha)}\frac{d^m}{dx^m}\int_a^x \frac{f(t)}{(x-t)^{-m+1+\alpha}}dt, & x>0,\ m-1\le\alpha<m, \\ f^m(x), & \alpha=m, \end{cases} $$

where $m = \lceil \alpha \rceil$ is the smallest integer such that $m > \alpha$ and d^m/dx^m denotes the standard derivatives of integer order.

Definition 3. The Caputo fractional derivative of $f(x)$ is:

$$ D^{\alpha}f(x) = \begin{cases} \frac{1}{\Gamma(m-\alpha)}\int_a^x \frac{f^{(m)}(t)}{(x-t)^{-m+\alpha+1}}dt, & x>0, m-1\le\alpha<m, \\ f^m(x), & \alpha=m. \end{cases} $$

The Caputo operator D^{α} advantages for fractional differential equations (FDEs) with initial conditions. The two definitions of Riemann-Liouville and Caputo are not equivalent and their relation is correlated by the following expression,

$$ {}^{R}D^{\alpha}f(x) = D^{\alpha}f(x) + \sum_{k=0}^{m-1} f^{(k)}(a)\Phi_{k-\alpha+1}(x-a). $$

$$ \Phi_{\alpha}(x) = \begin{cases} x^{\alpha-1}, & x>0, \\ 0, & x\le 0. \end{cases} $$

Definition 4. The left-sided mixed Riemann-Liouville integral of order $r = (r_1, r_2)$ for the function $u(x, y)$ is defined as

$$ (I_{\theta}^{r}u)(x,y) = \frac{1}{\Gamma(r_1)}\frac{1}{\Gamma(r_2)}\int_a^x\int_a^y (x-s)^{r_1-1}(y-t)^{r_2-1}u(s,t)dsdt, \tag{1} $$

where $r \in (0,\infty)\times(0,\infty)$, $\theta = (0,0)$ and $u \in L^1(J)$. So, we have the following:

(1) $(I_{\theta}^{\theta}u)(x,y) = u(x,y)$,

(2) $(I_{\theta}^{r}u)(x,y) = \int_a^x\int_a^y u(s,t)dsdt$ where $r = (1,1)$ *and for all* $(x,y)\in J$,

(3) $(I_{\theta}^{r}u)(x,0) = (I_{\theta}^{r}u)(0,y) = 0$ for $x\in[0,a]$, $y\in[0,b]$,

(4) Let λ, $\omega \in (-1,\infty)$ then $(I_{\theta}^{r}x^{\lambda}y^{\omega}) = \frac{\Gamma(\lambda+1)\Gamma(\omega+1)}{\Gamma(\lambda+r_1+1)\Gamma(\omega+r_2+1)}x^{\lambda+r_1}y^{\omega+r_2}$ for all $(x,y)\in J$.

For more information about the left-sided mixed Riemann-Liouville integral see also [20].

Two-dimensional fractional Volterra integral equation is difined as follows:

$$ u(x,y) - \frac{1}{\Gamma(r_1)}\frac{1}{\Gamma(r_2)}\int_a^x\int_a^y (x-s)^{r_1-1}(y-t)^{r_2-1}K(x,y,s,t,u(s,t))dsdt $$
$$ = g(x,y). \tag{2} $$

3. Discretization by LRBF-MQ

In this section, the local RBF method is used as a technique for approximation of boundary value problems and fractional integral equations . To illustrate the local RBF method, we consider the following boundary value problem:

$$\begin{cases} L(u(x)) = f(x), & x \in \Omega, \\ B(u(x)) = h(x), & x \in \partial\Omega, \end{cases} \tag{3}$$

where L and B denote the linear partial differential operator and boundary operation respectively. $\Omega \subset R^n$ is a bounded domain, and $\partial\Omega$ denotes its boundary. In the local RBF method, we consider a set of N scattered nodal points in the domain and on the boundary that is represented by $\Xi = \{x_k\}_{k=1}^{N}$. Then, to approximate the unknown solution u at an arbitrary point $x_k,\ k = 1, ..., N$, we consider a local region Ω_x around this point, called the domain of influence of point x_k, covering a number of n nodal points as shown in Fig.1. The solution

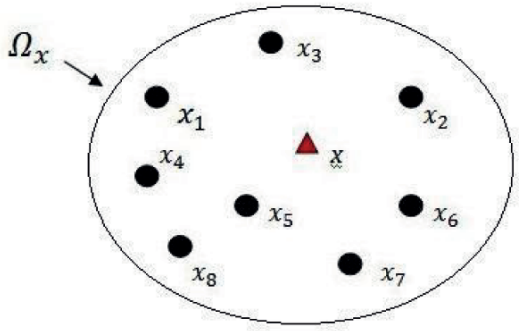

Figure 1. Influence domain Ω_x of a node x embracing 8 neighboring nodes.

$u(x)$ can be approximated by a localized formulation as follows:

$$\widetilde{u}(x) = \sum_{j=1}^{n} \lambda_j \phi_j(x), \tag{4}$$

where

$$\phi_j(x) = \sqrt{\|x - x_j\|^2 + c^2},$$

is the multiquadric(MQ), n is the number of nodal points fallen with in the influence domain Ω_x of x. The parameter $c > 0$ is known as the shape parameter, and describes the relative width of the RBFs around their centers. This parameter plays an important role for the accuracy of the method. In most articles, the authors choose this shape parameter by trial and error or some other techniques [21, 22]. Here the particle swarm optimization algorithm is applied to obtain the optimum value of this parameter which is explained in the next section.

To obtain the values of the coefficients λ_j, we can first evaluate Eq. (4) at all nodal points $x_i; i = 1, 2, ..., n$ in each influence domain. If all the collocation points are distinct, and $\phi(x)$ is a positive definite, it can be proved that the matrix $\Phi = (\phi(\|x_i^k - x_j^k\|_2))$ is non-singular. Hence, the unknown coefficients in Eq. (4) have the following matrix form:

$$\lambda^k = \Phi^{-1} u^k, \tag{5}$$

where $\lambda^k = (\lambda_1^k, \lambda_2^k, ..., \lambda_n^k)^T$, $u^k = (u(x_1^k), u(x_2^k), ..., u(x_n^k))^T$. Then the approximate solution $\widetilde{u}(x_k)$ can be revise according to the given nodal values $u(x_j^k)$ at influence domain x_k:

$$\widetilde{u}(x_k) = \Phi^k \lambda^k = \Phi^k \Phi^{-1} u^k = \Psi^k u^k, \tag{6}$$

where $\Phi^k = (\phi(\|x_k - x_j^k\|_2))$, and $\Psi^k = \Phi^k \Phi^{-1} = [\psi_1, \psi_1, ..., \psi_n]$. The functions $\psi_i,\ i = 1, 2, ..., n$ are called the shape functions for the local RBF interpolation. Fractional derivatives $D^\alpha \Psi$ can be computed as follows:

Using Eq (5),

$$D^\alpha(u(x)) = D^\alpha[\sum_{j=1}^{n} \lambda_j \phi_j(x)] = D^\alpha[\sum_{j=1}^{n} \Phi^{-1} \phi_j(x) \widetilde{u}] = [\Phi^{-1} D^\alpha(\Delta^k(x))]\widetilde{u}, \tag{7}$$

where $D^\alpha \Delta^k(x) = [D^\alpha \phi_1(x), D^\alpha \phi_2(x), ..., D^\alpha \phi_n(x)]$ and $\widetilde{u} = (\widetilde{u}(x_1), \widetilde{u}(x_2), ..., \widetilde{u}(x_n))$.

Finally, corresponding to each node, a local equation will be obtained and all these equations should be assembled in a global final system. When assembling the local equations in the final global system, the ith row of the global matrix is a vector with n non-zero elements $[0, ..., \vartheta(\psi_1), 0, ..., \vartheta(\psi_2), 0, ..., \vartheta(\psi_n), 0, ..., 0]$ in which $\vartheta(\psi_i)$ is equal either $L(\psi_i)$ or $B(\psi_i)$ depending on operator that acts on ψ_i. then Substituting these vectors into Eq. (3), yields

$$\begin{bmatrix} L\Psi \\ B\Psi \end{bmatrix} \widetilde{u} = [b],$$

which in general is the following system of equations:

$$Au = b.$$

Note that the number of columns, which ψ_k is located, is the global number of node k in all callocation node. In other words, this row is the extension of vector by patching zeros into entries associated with the nonselected $[\vartheta(\psi_1), \vartheta(\psi_2), ..., \vartheta(\psi_n)]$ nodes in the Ω_{x_i}.

By solving the above mentioned linear sparse system of equations, we get the approximate solutions $\widetilde{u}$ at all of the collocation points.

Similarly for two-dimensional fractional integral equation we have:

$$u(p) \simeq \sum_{\gamma=0}^{n} \lambda_\gamma \phi(\|p - p_\gamma\|) = \lambda^T \varphi(p), \tag{8}$$

then we have

$$\lambda = \varphi^{-1} u, \tag{9}$$

where $p = (x, y)$ and $p_\gamma = (x_\gamma, y_\gamma) \in R^2$. The dependence on the RBF expansion coefficients can be removed from Eq. (9) by the following:

$$u(p_k) \simeq \sum_{\gamma=0}^{n} \lambda_\gamma \phi(\|p_k - p_\gamma^s\|) = \Phi^k \lambda^k = \Phi^k \Phi^{-1} u^k = \Psi u^k, \tag{10}$$

substituting Eqs. (9) and (10) in Eq. (2) we have:

$$\begin{aligned} &\Psi u^k - \frac{1}{\Gamma(r_1)\Gamma(r_2)} \int_a^x \int_a^y (x-s)^{r_1-1}(y-t)^{r_2-1} \\ &\cdot K(x, y, s, t, \Phi^{-1}\phi(s,t)\widetilde{u}) ds dt = g(x, y). \end{aligned} \tag{11}$$

Substituting the given collocation points in the above equation and applying Legendre quadrature integration formula, we obtain

$$\begin{aligned} &\Psi \widetilde{u} - \frac{1}{\Gamma(r_1)\Gamma(r_2)} \sum_{k=0}^{m} \sum_{l=0}^{m} w_k w_l (x_i - \xi_k)^{r_1-1}(y_j - \tau_l)^{r_2-1} \\ &\cdot K(x_i, y_j, \xi_k, \tau_j, \Phi^{-1}\phi(\xi_k, \tau_l)\widetilde{u}) = g(x_i, y_j). \end{aligned} \tag{12}$$

4. Choosing a Shape Parameter

In RBFs interpolation, different shape parameters correspond to different approximation results. In this section presented particle, swarm optimization algorithm (PSO) for optimizing shape parameters with respect to error in an global and local RBF interpolation is applied.

4.1 Particle swarm optimization algorithm (PSOA)

PSOA was firstly proposed by Eberhart and Kennedy (1995) based on the population (swarm) of particles [23]. Each particle is associated with velocity that indicates where the particle is traveling. The process is such that a group of particles in the particle swarm optimization algorithm are initially created randomly and by updating the generations, they try to find the optimal solution. In a bunch of N particles, the position of the ith particle in the search space is located under the influence of a n-dimensional spatial vector of Eq.(13).

$$X_i = (x_{i1}, x_{i2}, ..., x_{in})^T \in S, \tag{13}$$

The velocity vector of this particle is as Eq. (14).

$$V_i = (v_{i1}, v_{i2}, ..., v_{in})^T \in S, \tag{14}$$

The best position of the ith particle is represented by the Eq. (15).

$$P_{besti} = (P_{besti1}, P_{besti2}, ..., P_{bestin})^T \in S. \tag{15}$$

In each step, each particle is updated using the two best values. First situation is the best one that a particle can achieve so far. This position is known and stored as P_{BEST}. The best alternative used by the algorithm is the best situation ever achieved by the particle population. The other most appropriate value used by the algorithm, the best position ever has been achieved by the particle population. this position is shown by G_{BEST}. After finding the best values, the speed and location of each particle is updated using Eqs. (16) and (17).

$$V_{i,t+1} = \omega V_{i,t} + c_1 r_1 (P_{i,t}^{best} - X_{i,t}) + c_2 r_2 \tag{16}$$

$$X_{i,t+1} = X_{i,t} + V_{i,t+1}. \tag{17}$$

$V_{i,t}$ and $X_{i,t}$ are respectively the velocity vectors and the position of the particle i in the repetition t. ω is a stationary coefficient 1 and 2 are acceleration coefficients the implementation of optimization algorithm particles are usually considered 2. Also r_1 and r_2 are two nonlinear stochastic numbers between 0 and 1. The condition for stopping the PSO algorithm is usually considered to be such that, if the difference between two consecutive results is less than a certain value, the algorithm is stopped or a certain number of repetitions are considered for the algorithm [24].

Here, the error is considered to be the objective function, and we find the optimal shape parameter by finding the least error in the repetitions of the PSO algorithm.

LRBF implementation.

The step-wise procedure for the implementation of LRBF collocation method is as follows:

Step 1: Selection of scattered nodal points in the domain and on the boundary.

Step 2: Consider a local region around each collocate point, called the domain of influence including the point itself and $n-1$ other points.

Step 3: Applying local interpolation on each subdomain, Upon computing Φ^{-1}, the coefficient vector calculated by $\lambda^k = \Phi^{-1} u^k$.

Step 4: Approximated function, $u(x_k)$, (x_k is center subdomain) expressed in terms of the nodal values at each subdomain. That is $\widetilde{u}(x_k) = \Psi^k u^k$.

Step 5: Finally,corresponding to each node a local equation will be obtained and all these equations should be assembled in a final global system.

Step 6: Finding the optimal shape parameter with the pso algorithm.

Step 7: Solving linear sparse system of equations, we get the approximate solutions u at all of the collocation points.

5. Numerical experiment

Test problems that we consider in this section consist of fractional integro-differential equation with the nonlocal boundary conditions, Bagley-Torvik equation and two-dimensional Volterra integral equation of fractional order. Accuracies of the numerical results are measured by infinity norm error $\|e\|_\infty$ or root mean square (RMS) error defined by:

$$\delta_{er} = \|e\|_\infty = \max\{|u_N(x_i) - u^*(x_i)|\}, \qquad x_i \in X,$$

and

$$RMS = \left(\sum_{z_i \in Z} \frac{(u_N x_i - u^*(x_i))^2}{|X|} \right)^{1/2},$$

where u_N is the numerical solution, u^* is the exact solution and X is the number of testing nodes.

Remark. 1) Number of infuence domain points is selected based on the factors of accuracy and cost of calculations.

2) In PSO, population size is set to 10 and maximum number of iterations is selected 100.

3) The method is implemented in MATLAB and the numerical experiments are performed using a laptop with an Intel(R) Core(TM) i5-3230M, CPU 2.60GHz, and 4 GB RAM.

5.1 Example 1.

Consider the following fractional integro-differential equation [19].

$$(18) \qquad {}^R D^{\frac{5}{4}} u(x) = (cosx - sinx)u(x) + f(x) + \int_0^x sintu(t),$$

with the nonlocal conditions

$$u(0) + u(1) + (\frac{e+1}{e+2})u'(0) + \frac{1}{2}u'(1) - 8\int_0^1 tu(t) = 0,$$
$$2u(0) + 2u(1) + (\frac{e}{e+1})u'(0) - u'(1) = 0.$$

By choosing $f(x) = \frac{8}{3}\frac{x^{\frac{3}{4}}}{\Gamma(\frac{3}{4})} - 2\cos x - 2x\sin x + x^2 \sin x + 2$, the exact solution of above problem is $u(x) = x^2$.

Numerical results versus the numbers of nodal points and stencil with optimal shape parameter are shown in Tabel 1. Fig. 2 presents the RMS error versus the number of the nodal points and stencil with optimal shape parameter. Fig. 3 shows the error curves for local and global RBF methods with 100 nodal points and optimal shape parameter. According to Tabel 1 and Figures 2 and 3, the local method is often just as accurate as the global RBF method.

Table 1: Numerical results with different number of nodal points by optimal neighborhood node and optimal shape parameter c and CPU time (seconds) for Ex.1.

		LRBF			GRBF		
N	n	δ_{er}	RMS	CPU(s)	δ_{er}	RMS	CPU(s)
20	7	1.33×10^{-4}	8.9799×10^{-4}	1.80	5.44×10^{-3}	2.5962×10^{-3}	4.17
30	7	5.45×10^{-4}	1.4264×10^{-4}	1.97	4.04×10^{-3}	1.7907×10^{-3}	5.67
50	11	3.38×10^{-4}	8.6699×10^{-5}	3.50	4.08×10^{-3}	1.7942×10^{-3}	12.12
80	16	1.36×10^{-4}	6.9852×10^{-5}	6.23	4.04×10^{-3}	2.0904×10^{-3}	26.13
100	17	5.85×10^{-5}	3.7125×10^{-5}	8.41	4.24×10^{-3}	2.7614×10^{-3}	39.30
150	21	8.18×10^{-5}	2.1590×10^{-5}	14.99	4.13×10^{-3}	2.2810×10^{-3}	85.90
200	25	5.45×10^{-5}	2.9491×10^{-5}	23.22	4.16×10^{-3}	1.7991×10^{-3}	149.35
250	32	3.84×10^{-4}	2.0969×10^{-4}	36.58	4.17×10^{-3}	4.0903×10^{-3}	239.13
300	35	2.92×10^{-4}	8.4034×10^{-5}	48.24	4.49×10^{-3}	4.2043×10^{-3}	339.24

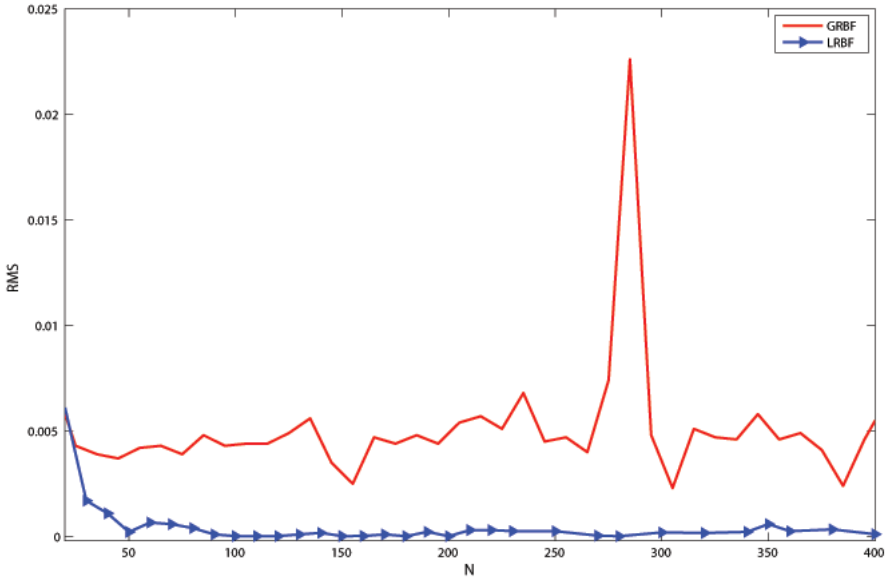

Fig. 2. RMS error versus N for Ex. 1.

5.2 Example 2.

Consider the following Bagley-Torvik equation [25]

$$u^{(2)}(x)+\theta D^{\alpha}u(x)+\sigma u(x) = f(x), \tag{19}$$

where

$$f(x) = (\lambda-1)(\lambda x-\lambda+2)x^{\lambda-3}+\theta\frac{(\lambda-1)!}{\Gamma(\lambda-\alpha)}(\frac{\lambda x}{\lambda-\alpha}-1)x^{\lambda-\alpha-1}+\sigma x^{\lambda-1}(x-1).$$

The exact solution for various values of $\theta = 0.5$, $\sigma = 1$ and $\lambda = 5$ and $\alpha = 0.3$ is $u(x) = x^{\lambda-1}(x-1)$.

Results for different values of the nodal points and the optimal stencil shown in the Table 2. Fig.4 presents the RMS error versus the number of the nodal points and Also, exact solution and approximate solution for various values α

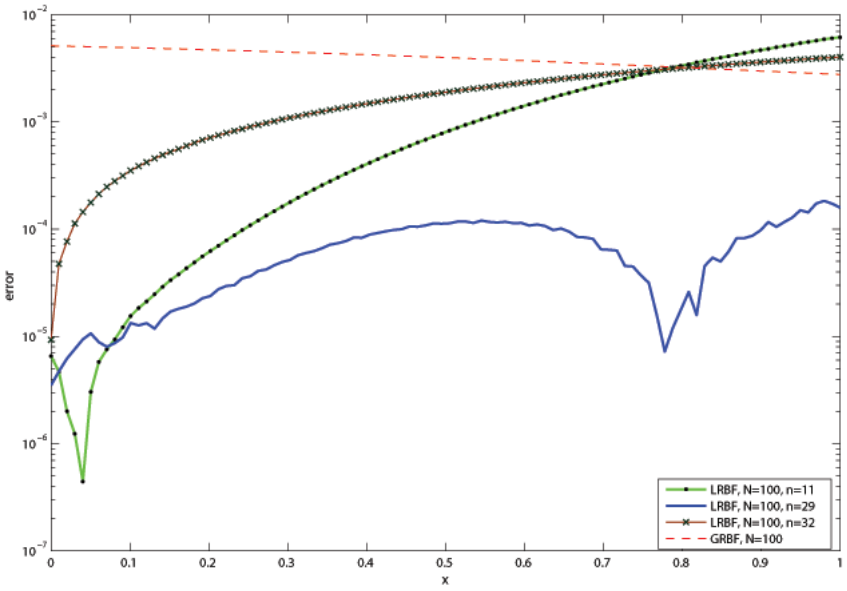

Fig. 3. Absolute errors for local and global RBF methods with optimal shape parameter for Ex.1.

Table 2: Numerical results with different number of nodal points and optimal shape parameter c for Ex.2.

		LRBF		GRBF	
N	n	δ_{er}	RMS	δ_{er}	RMS
30	9	4.9909×10^{-4}	2.0626×10^{-4}	9.8453×10^{-5}	9.8248×10^{-5}
50	12	8.9333×10^{-5}	1.2044×10^{-5}	4.4596×10^{-5}	4.4521×10^{-6}
80	16	6.2402×10^{-5}	2.5866×10^{-6}	1.3771×10^{-6}	3.3757×10^{-6}
100	19	5.5600×10^{-6}	6.2525×10^{-7}	2.4027×10^{-6}	2.4027×10^{-6}
150	39	5.7572×10^{-6}	8.9533×10^{-7}	1.2282×10^{-6}	1.1645×10^{-6}
200	35	6.3928×10^{-5}	5.7164×10^{-6}	1.1907×10^{-6}	1.0134×10^{-6}
250	26	1.2551×10^{-5}	2.0264×10^{-5}	2.2545×10^{-5}	1.5756×10^{-6}
300	33	8.0320×10^{-5}	3.6287×10^{-4}	2.1676×10^{-5}	1.4436×10^{-5}

presented in Fig. 5. Table 2 Shows that for the less number of collocation points, global RBFs method is better than local RBF method, but with increasing collocation points, the performance of the local RBFs method is better [25].

5.3 Example 3.

Consider the following Bagley-Torvik equation [26].

$$u^{(2)}(x)+\theta D^{\alpha}u(x) = -1-e^{(x-1)}, \quad (20)$$

In general, the exact solution of the problem is not known. However, for $\alpha = 1$, $\theta = -1$, the problem has exact solution is $u(x) = x(1 - e^{x-1})$.

Table 3 shows the numerical results at different the numbers of nodal points and stencil with optimal shape parameter. Approximate solutions with various α are presented in Fig. 6. RMS error and absolute error versus the number of the nodal points are shown in Fig. 7. Considering the results, accuracy of the

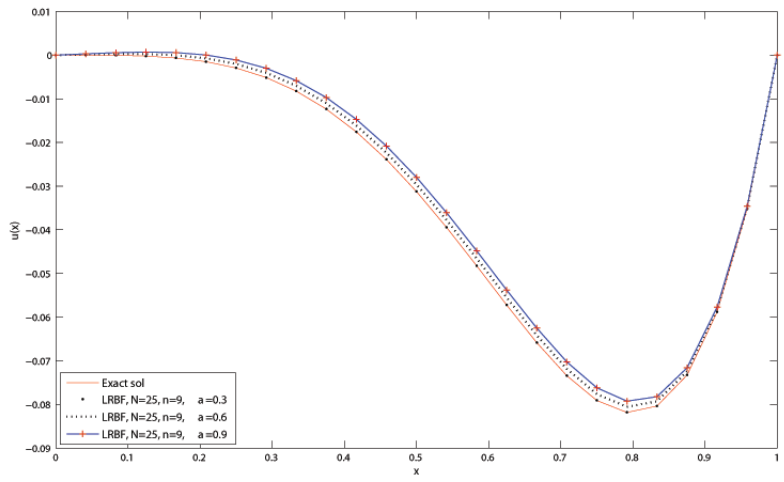

Fig. 4. Approximate solution obtained for Ex.2.

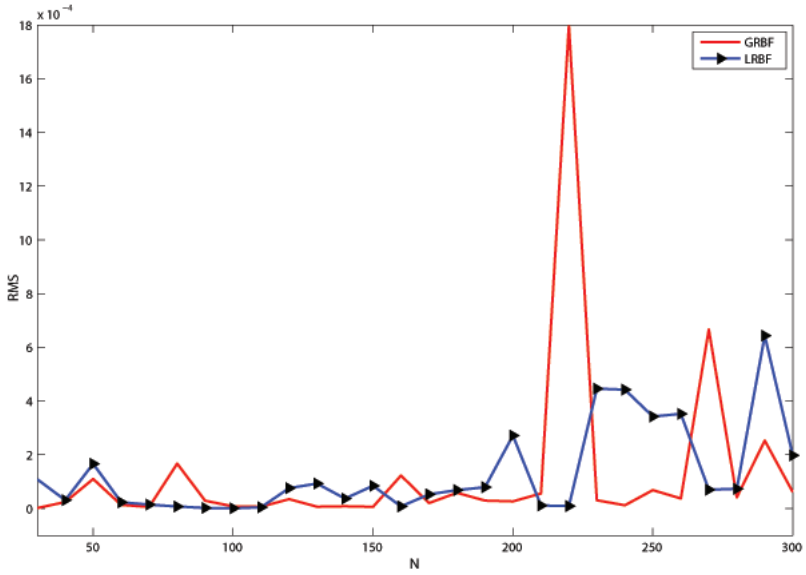

Fig. 5. RMS error versus N for Ex.2.

local method is more than the global method, and the local method is faster. Better result is obtained with local RBF collocation method than the method of [25].

Tabels 1 to 3 show that one of the advantages of using the optimal shape parameter in the local and global RBFs methods is that the approximate values obtained do not oscillate for the number of different nodal points.

Table 3: Numerical results with different number of nodal points and optimal shape parameter c for Ex.3.

		LRBF		GRBF	
N	n	δ_{er}	RMS	δ_{er}	RMS
20	6	3.7348×10^{-7}	4.4256×10^{-7}	4.9140×10^{-7}	1.9437×10^{-7}
30	6	3.0022×10^{-7}	1.7868×10^{-7}	7.5015×10^{-7}	2.2452×10^{-7}
50	6	1.5166×10^{-7}	6.9974×10^{-8}	1.9361×10^{-7}	8.5469×10^{-8}
80	11	1.3692×10^{-7}	2.5266×10^{-8}	3.1795×10^{-6}	1.0485×10^{-6}
100	20	1.1811×10^{-7}	1.9041×10^{-8}	8.5846×10^{-6}	3.1034×10^{-6}
150	21	3.0144×10^{-7}	2.5230×10^{-8}	9.0405×10^{-6}	2.2476×10^{-6}
200	21	4.5467×10^{-7}	4.7993×10^{-7}	3.0446×10^{-6}	1.9750×10^{-6}
250	21	4.6912×10^{-6}	1.2645×10^{-7}	1.0388×10^{-6}	1.6379×10^{-6}

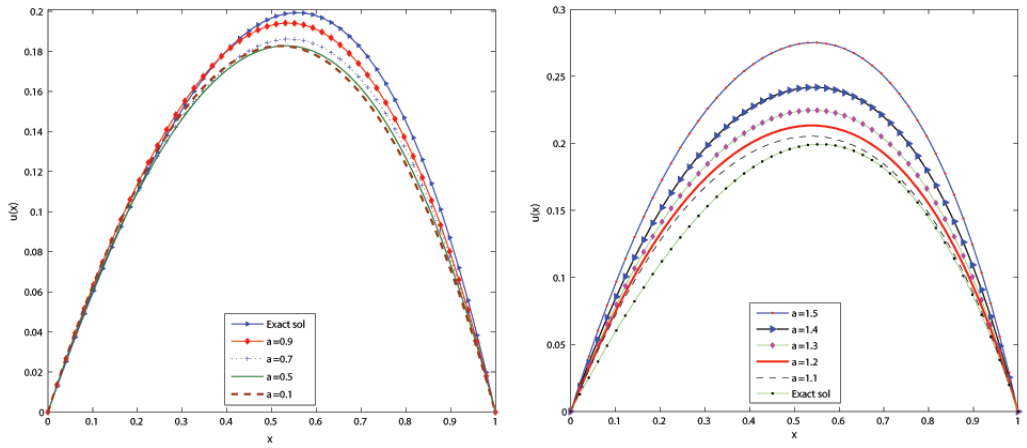

Fig. 6. Numerical solutions of Ex.3 for various α.

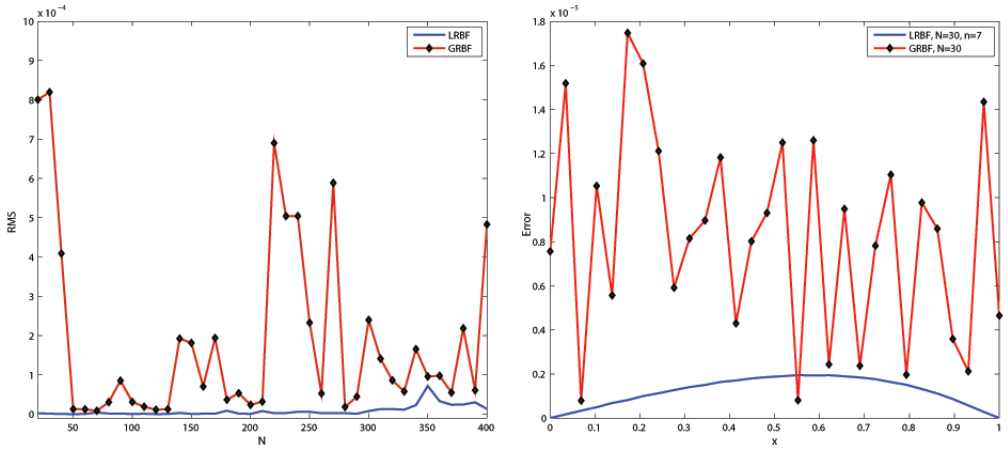

Fig. 7. RMS errors and abselot error local and global RBF methods for Ex.3.

5.4 Example 4.

Consider the following two-dimensional nonlinear fractional Volterra integral equation:

$$u(x,y) - \frac{1}{\Gamma(\frac{3}{2})\Gamma(\frac{5}{2})}\left[\int_0^x \int_0^y (x-s)^{\frac{1}{2}}(y-t)^{\frac{3}{2}}\sqrt{xyt}[u(s,t)]^2 dtds\right]$$

$$= \sqrt{y}\left(\frac{-1}{180}x^3 y^{\frac{7}{2}} + \sqrt{\frac{x}{3}}\right), \tag{21}$$

Table 4: Numerical results obtained with different number of nodal points for Ex.4.

	3×3 stencil			5×5 stencil		
N	δ_{ex}	RMS	CPU(s)	δ_{ex}	RMS	CPU(s)
6^2	1.042×10^{-2}	5.8280×10^{-3}	127.5	8.5×10^{-2}	3.5273×10^{-3}	343.2
7^2	2.872×10^{-2}	1.2000×10^{-3}	188.2	4.6×10^{-2}	2.9653×10^{-3}	495.5
8^2	1.107×10^{-2}	3.6457×10^{-4}	311.1	3.0×10^{-3}	3.6065×10^{-4}	663.9
9^2	1.480×10^{-3}	2.6248×10^{-4}	534.0	2.9×10^{-3}	9.5724×10^{-4}	1603.0
10^2	2.072×10^{-4}	8.6700×10^{-5}	827.9	5.1×10^{-3}	3.3647×10^{-4}	2042.3
11^2	3.421×10^{-4}	9.2053×10^{-5}	961.5	4.2×10^{-2}	3.2812×10^{-3}	2973.6

In which the exact solution is $u(x, y) = \frac{\sqrt{3xy}}{3}$. The results with optimal shape parameter are presented in Table 4. Fig. 8 show the cross section of the approximate solutions with $N = 10^2$, 3×3 stencils and fixed values of y. The results obtained in Test problems (4) with local RBF method are more accurate than the results obtained in [27].

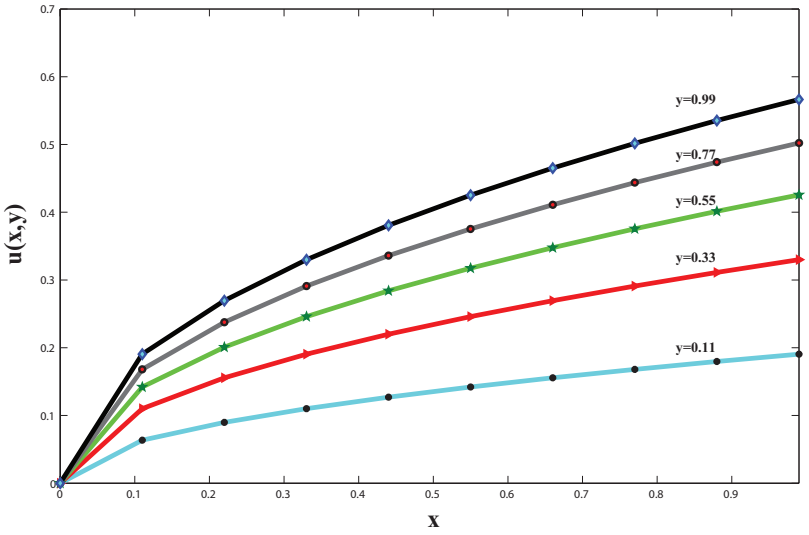

Fig. 8. Cross section of approximate solution obtained with $N = 10^2$ and 3×3 stencils for Ex. 4

5.5 Example 5.

Consider the two-dimensional fractional Volterra integral equation:

$$u(x, y) - \frac{1}{\Gamma(r_1)\Gamma(r_2)} \int_0^x \int_0^y (x - s)^{r_1 - 1} (y - t)^{r_2 - 1} \sqrt{xy} stu(s, t) ds dt = f(x, y),$$

$$f(x, y) = x^3(y^2 - y) - \frac{1}{60} x^{\frac{11}{2}} y^{\frac{7}{2}} (3y - 4).$$

We applied the presented method for various values of r_1 and r_2. For $r_1 = r_2 = 1$, the exact solution is given as $u(x, y) = x^3(y^2 - y)$. Note that as r_1 and r_2 approach to 1, the numerical solution converges to the analytical solution $u(x, y) = x^3(y^2 - y)$. Table 5 compares the absolute errors with 100 number of nodal points, 3×3 stencil between the local RBFs method and method [28].

Table 5: Numerical results obtained with 100 number of nodal points, with 3×3 and optimal shape parameter c for Ex.5.

	$r_1 = r_2 = 0.8$		$r_1 = 0.8,\ r_2 = 0.95$	
x=y	δ_{er}	Error [28]	δ_{er}	Error [28]
0.0	0.0	3.544×10^{-4}	0.0	3.068×10^{-3}
0.1	8.4684×10^{-7}	1.388×10^{-3}	1.2140×10^{-6}	1.240×10^{-3}
0.2	1.1030×10^{-7}	8.772×10^{-4}	4.5487×10^{-5}	1.166×10^{-3}
0.3	1.6701×10^{-6}	1.407×10^{-3}	4.0259×10^{-4}	1.863×10^{-3}
0.4	2.0687×10^{-5}	1.153×10^{-3}	9.4018×10^{-4}	5.133×10^{-3}
0.5	1.2684×10^{-5}	5.673×10^{-3}	1.2354×10^{-3}	4.848×10^{-3}
0.6	4.8970×10^{-4}	9.748×10^{-3}	2.1018×10^{-3}	8.742×10^{-3}
0.7	1.2566×10^{-4}	1.089×10^{-3}	2.9120×10^{-3}	9.716×10^{-3}
0.8	1.3564×10^{-3}	7.730×10^{-3}	3.3028×10^{-3}	6.411×10^{-3}
0.9	3.4802×10^{-3}	1.222×10^{-3}	4.2901×10^{-3}	2.162×10^{-4}

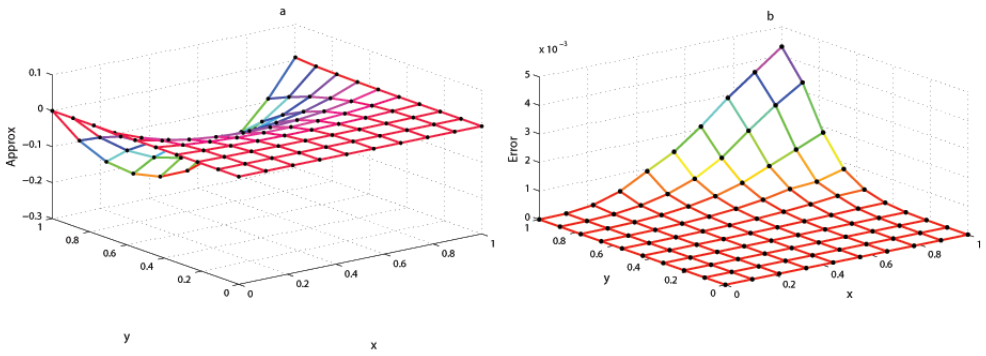

Fig. 9. Graphs of approximate solution (a) and absolute error (b) with $r_1 = 0.8$ and $r_2 = 0.95$ for Ex.5.

Graphs of approximate solution and absolute error with $r_1 = 0.8$, $r_2 = 0.95$, $N = 100$ and 3×3 stencil are given in Fig. 9. The results obtained in this paper, with local RBF method are more accurate than the results obtained in [28].

6. Conclusion

A meshless local RBF method was proposed to solve fractional integro-differential equation and two-dimensional fractional Volterra integral equation. In one-dimensional problems, by increasing the number of collocation points to find an optimal and more stable response, the number of nodes in local domain of influence increases. Numerical results showed that in the two dimensional fractional integral equations the local RBF method is much more efficient than the global RBF method, so, it can be concluded that local RBF method is more suitable for high dimensional problems.

The effectiveness of the method has the following reasons:

1) The use of the strong form equation and collocation approach made the method simpler than similar methods.

2) Using the locallization approach, the matrix operations required only the inversion of matrices of small size and the final global matrix became sparse.

So the method is suitable for large-scale and complicated problems.

References

[1] Z. O. T. R. Onate E, S. Idelsohn, *Numerical Methods in Engineering*, 39 (1996), 38393866.

[2] P. Assari, M. Dehghan, *A meshless discrete collocation method for the numerical solution of singular-logarithmic boundary integral equations utilizing radial basis functions*, Applied Mathematics and Computation, 315 (2017), 424444.

[3] L. Sun, W. Chen, C. Zhang, *A new formulation of regularized meshless method applied to interior and exterior anisotropic potential problems*, Applied Mathematical Modelling, 37 (2013), 74527464.

[4] A. Shirzadi, L. Ling, S. Abbasbandy, *Meshless simulations of the two-dimensional fractional-time convection-diffusion-reaction equations*, Eng. Anal. Bound. Elem., 36 (2012), 15221527.

[5] A. Shirzadi, L. Ling, *Convergent overdetermined-RBF-MLPG for solving second order elliptic PDEs*, Advances in Applied Mathematics and Mechanics, 5 (2013), 7889.

[6] S. Abbasbandy, A. Shirzadi, *Mlpg method for two-dimensional diffusion equation with neumann's and non-classical boundary conditions*, Applied Numerical Mathematics, 61 (2011), 170180.

[7] A. Shirzadi, *Solving 2D reaction-diffusion equations with nonlocal boundary conditions by the RBF-MLPG method*, Computational Mathematics and Modeling, 25 (2014), 521529.

[8] A. Shirzadi, F. Takhtabnoos, *A local meshless method for cauchy problem of elliptic pdes in annulus domains*, Inverse Problems in Science and Engineering, 0 (2015), 115.

[9] A. Shirzadi, F. Takhtabnoos, *A local meshless collocation method for solving Landau-Lifschitz-Gilbert equation*, Eng. Anal. Bound. Elem., 61 (2015), 104113.

[10] E. Shivanian, *On the convergence analysis, stability, and implementation of meshless local radial point interpolation on a class of three-dimensional wave equations*, International Journal for Numerical Methods in Engineering, 105 (2016), 83110.

[11] V. R. Hosseini, E. Shivanian, W. Chen, *Local radial point interpolation (mlrpi) method for solving time fractional diffusion-wave equation with damping*, Journal of Computational Physics, 312 (2016), 307332.

[12] G. L. Belytschko T, Lu YY, *Element-free galerkin methods*, Int. J. Numer. Meth. Engrg., 37 (1994), 229256.

[13] C. K. Lee, X. Liu, S. C. Fan, *Local multiquadric approximation for solving boundary value problems*, Computational Mechanics, 30 (2003), 396409.

[14] M. Li, W. Chen, C. Chen, *The localized RBFs collocation methods for solving high dimensional PDEs*, Engineering Analysis with Boundary Elements, 37 (2013), 1300 1304.

[15] F. Takhtabnoos, A. Shirzadi, *A new implementation of the finite collocation method for time dependent PDEs*, Eng. Anal. Bound. Elem., 63 (2016), 114124.

[16] E. J. Kansa, *Multiquadricsa scattered data approximation scheme with applications to computational fluid-dynamicsi surface approximations and partial derivative estimates*, Computers and Mathematics with Applications, 19 (1990), 127145.

[17] E. J. Kansa, *Multiquadricsa scattered data approximation scheme with applications to computational fluid-dynamicsii solutions to parabolic, hyperbolic and elliptic partial differential equations*, Computers and Mathematics with Applications, 19 (1990), 147161.

[18] I. Podlubny, *Fractional differential equations*, Mathematics In Science And Engineering, 1999.

[19] D. Nazari, S. Shahmorad, *Application of the fractional differential transform method to fractional-order integro-differential equations with nonlocal boundary conditions*, Journal of Computational and Applied Mathematics 234 (2010), 883891.

[20] O. SM., *Efficient algorithms with neural network behaviour*, J. Complex Syst., 1 (1987), 273347.

[21] G. E. Fasshauer, J. Zhang, *On choosing "optimal" shape parameters for rbf approximation*, 45 (2007), 345368.

[22] J. Wang, G. Liu, *On the optimal shape parameters of radial basis functions used for 2-d meshless methods*, Computer Methods in Applied Mechanics and Engineering, 191 (2002), 26112630.

[23] J. Kennedy, R. Eberhart, *Particle swarm optimization, in neural networks*, IEEE International Conference on, Nov/Dec, 1995 (1995), 19421948.

[24] A. J. Choobbasti, H. Tavakoli, S. S. Kutanaei, *Modeling and optimization of a trench layer location around a pipeline using artificial neural networks and particle swarm optimization algorithm*, Tunnelling and Underground Space Technology, 40 (2014), 192202.

[25] W. Zahra, M. V. Daele, *Discrete spline methods for solving two point fractional bagleytorvik equation*, 296 (2017), 4256.

[26] M. ur Rehman, R. A. Khan, *A numerical method for solving boundary value problems for fractional differential equations*, Applied Mathematical Modelling, 36 (2012), 894907.

[27] S. Najafalizadeh, R. Ezzati, *Numerical methods for solving two-dimensional nonlinear integral equations of fractional order by using two-dimensional block pulse operational matrix*, Applied Mathematics and Computation, 280 (2016), 4656.

[28] M. Asgari, R. Ezzati, *Using operational matrix of two-dimensional bernstein polynomials for solving two-dimensional integral equations of fractional order*, Applied Mathematics and Computation, 307 (2017), 290298.

Accepted: 11.05.2018